


Robust thresholdlike effect of internal noise on stochastic resonance in an organic field-effect transistor

Yoshiharu Suzuki and Naoki Asakawa*

Graduate School of Science and Technology, Gunma University, 1-5-1 Tenjincho, Kiryu, Gunma 376-8515, Japan

 (Received 11 November 2017; revised manuscript received 9 January 2018; published 26 January 2018)

The application of noise to a nonlinear system can have the effect of increasing the signal transmission of the system through the phenomenon of stochastic resonance (SR). This paper presents an analytical characterization of the dependence of the signal transmission performance of an organic field-effect transistor (OFET) on external noise. Similarly to the threshold of a nonlinear system, the additive internal noise of the system can be used to control the emergence of SR. Internal noise or the addition of random numbers to the system enables one to observe the SR phenomenon in an OFET under an intrinsically nonresonant condition. Internal noise plays a thresholdlike role, but it functions in a different manner. The fluctuations in performance due to external noise become smaller when the effect of internal noise becomes dominant compared with that of the threshold. In conclusion, it is found that internal noise plays a robust thresholdlike role with respect to variations in external noise intensity.

DOI: [10.1103/PhysRevE.97.012217](https://doi.org/10.1103/PhysRevE.97.012217)

I. INTRODUCTION

Although, in general, noise interferes with the functions of systems and degrades their performance, signal transmission performance in nonlinear systems can be enhanced by noise through a phenomenon called stochastic resonance (SR) [1,2]. SR has been observed in several biological systems, and is associated with bio-inspired signal processing [3–7]. This counterintuitive phenomenon may possibly allow information processing with ultralow energy consumption. Furthermore, SR occurs in some artificial systems, including organic field-effect transistors (OFETs) [8], GaAs nanowire transistors [9,10], Si nanowire transistors [11], carbon nanotube transistors [12–15], and VO₂ devices [16]. OFETs, in particular, are candidates as scalable devices for applications taking advantage of SR, with the latter being generated by intrinsic noise due to fluctuating electrical characteristics of a polymer semiconductor instead of by external noise [8,17].

We have previously reported that internal noise in the dielectric layer of an OFET suppresses the fluctuations in signal transmission performance associated with variations in the intensity of applied external noise [8]. We have called this property a *noise-robustness* effect against external noise. Although the signal enhancement by SR is weak, this robustness allows a broader optimal range of external noise intensity for the emergence of SR. This effect, as well as the independent effect of a parallel circuit arrangement of device elements presented by Collins *et al.* [2], allow a system to maintain stable performance with respect to external noise fluctuations.

The generation of SR in a threshold-free system has been discussed previously [18,19], and it has been shown that internal noise promotes SR in a nonlinear system even in the absence of a threshold [18]. However, so far, there have been no studies of SR in a single device element in the

presence of internal noise in which the focus has been on the signal-to-threshold distance, which is a significant factor governing the emergence of SR. A suprathreshold signal is not enhanced by external noise except in the cases of a nonlinear system based on a multiple parallel network [20] and a single bistable dynamic system involving a synchronization loss mechanism [21]. Therefore, in this paper, by considering OFET characteristics, we shall discuss the thresholdlike role of internal noise in SR, comparing it with the conventional threshold. Furthermore we shall also evaluate the robustness effect against external noise.

II. MODEL DESCRIPTION

In a nonlinear response system comprising a common-drain circuit with an OFET, SR has been observed on application of external noise [8]. This system is also subject to internal noise with a voltage-independent constant intensity, and its output y can be modeled by

$$y(t) = \begin{cases} -A(x(t) + \xi(t) - \theta)^2 + \eta(t) & (x(t) + \xi(t) < \theta), \\ \eta(t) & (\text{otherwise}), \end{cases} \quad (1)$$

where $x(t)$, θ , and A are the input signal value (depending on time t), the threshold, and a constant fitting parameter of the system, respectively. The random variables $\xi(t)$ and $\eta(t)$ are the external and internal noises, of which autocorrelation functions are $\langle \xi(t)\xi(t') \rangle = \sigma_\xi^2 \delta(t - t')$ and $\langle \eta(t)\eta(t') \rangle = \sigma_\eta^2 \delta(t - t')$, respectively [$\delta(t)$ is the Dirac delta function]. In this model, a negative input voltage puts the device into the ON state, since the OFET is a p -channel device and a common-drain circuit is a noninverted system. Here, we assume that the input signal is a pulse wave for consistency with the previous experiments. Additionally, θ , A , and the intensities of the noises ξ and η are normalized by the intensity of the input signal value. Owing to this normalization, x should be 1 or -1 with probability D and $1 - D$, respectively. We also made assumptions that external

*Corresponding author: asakawa@gunma-u.ac.jp

noise ξ and internal noise η are independent Gaussian random variables with zero mean, strictly stationary and ergodic. In this paper, the correlation coefficient ρ for input x and output y is taken as a measure of signal transmission performance and is defined as

$$\rho = \frac{\text{cov}[x, y]}{\sqrt{\text{var}[x] \text{var}[y]}}, \quad (2)$$

where $\text{cov}[\cdot]$ is the covariance and $\text{var}[\cdot]$ is the variance. As derived in Appendix B, the analytical expression for the correlation coefficient has the form

$$\rho = -D(1-D)(E_+ - E_-) \times \left[D(1-D) \left(E_{2+}D + E_{2-}(1-D) + \frac{\sigma_\eta^2}{A^2\sigma_\xi^4} - [E_+D + E_-(1-D)]^2 \right) \right]^{-1/2}, \quad (3a)$$

with

$$E_\pm = \frac{1}{\sqrt{2\pi\sigma_{\theta\pm}^2}} \exp\left(-\frac{1}{2\sigma_{\theta\pm}^2}\right) + \frac{1 + \sigma_{\theta\pm}^2}{2\sigma_{\theta\pm}^2} \left[1 + \text{erf}\left(\frac{1}{\sqrt{2\sigma_{\theta\pm}^2}}\right) \right], \quad (3b)$$

$$E_{2\pm} = \frac{1 + 5\sigma_{\theta\pm}^2}{\sqrt{2\pi\sigma_{\theta\pm}^6}} \exp\left(-\frac{1}{2\sigma_{\theta\pm}^2}\right) + \frac{1 + 6\sigma_{\theta\pm}^2 + 3\sigma_{\theta\pm}^4}{2\sigma_{\theta\pm}^4} \left[1 + \text{erf}\left(\frac{1}{\sqrt{2\sigma_{\theta\pm}^2}}\right) \right], \quad (3c)$$

$$\sigma_{\theta\pm}^2 = \left(\frac{\sigma_\xi}{\mp 1 + \theta} \right)^2, \quad (3d)$$

in the case of nonzero external noise intensity $\sigma_\xi \neq 0$, where erf is the error function [$\text{erf}(z) = 2 \int_0^z \exp(-t^2) dt / \sqrt{\pi}$]. $\sigma_{\theta\pm}^2$ is the variance of external noise normalized by the signal-to-threshold distance. When σ_ξ is zero, the correlation coefficient is

$$\rho_0 = \begin{cases} 0 & (\theta \leq -1), \\ \frac{(-1-\theta)^2 D(1-D)}{\sqrt{D(1-D)[(-1-\theta)^4(1-D)D + \frac{\sigma_\eta^2}{A^2}]}} & (-1 < \theta \leq 1), \\ \frac{4\theta D(1-D)}{\sqrt{D(1-D)[16\theta^2(1-D)D + \frac{\sigma_\eta^2}{A^2}]}} & (1 < \theta). \end{cases} \quad (4)$$

The influence of internal noise on the correlation coefficient is dominated by σ_η^2/A^2 , as can be seen from Eqs. (3a) and (4), and internal noise affects system performance when A is small. The fitting parameter A is determined from the carrier mobility of the OFET, and, in most cases, is smaller in OFETs than in inorganic transistors ($A = 3.0 \times 10^{-6} \text{ V}^{-1}$ in the fabricated OFET described in [8]). Although white noise is assumed here, Hooge's constant α_H , which is the relative noise at 1 Hz in f^{-1}

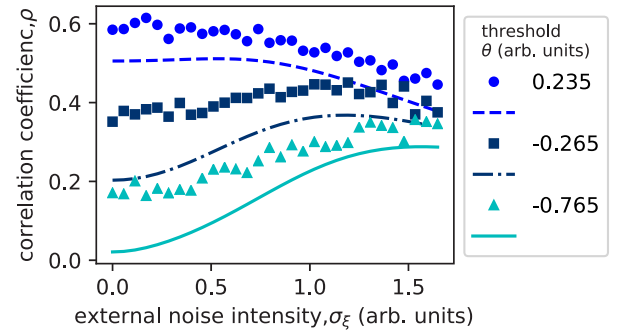


FIG. 1. Variation of the correlation coefficient between input and output signals as a function of external noise intensity for various thresholds. Symbols represent the averaged value of the correlation coefficient calculated from experimental data from four trials under identical conditions using the fabricated OFET, and solid lines represent the analytical value from Eqs. (3) and (4). In the experiments, the threshold was changed by an input dc bias at the input signal voltage $x = \pm 4 \text{ V}$ and a duty ratio $D = 80\%$. Parameters, normalized by the input signal intensity, are an internal noise intensity $\sigma_\eta = 1.25 \times 10^{-5}$ and a fitting parameter $A = 1.2 \times 10^{-5}$.

noise [22], is larger in organic than in inorganic devices (e.g., it is in the range 4–50 for a polymer FET [22] but only about 10^{-3} for an amorphous-silicon thin-film transistor [23]). Therefore, the effect of internal noise is expected to be greater in an OFET.

Figure 1 shows the correlation coefficient as a function of external noise intensity according to Eqs. (3) and (4). The results of the corresponding experiments using the fabricated OFET are also plotted. In the experiments, the threshold value was changed by the imposition of an input dc bias on the input signal (see Appendix A and the previous paper [8] for experimental details). The correlation coefficient increases with increasing external noise intensity for normalized thresholds (dimensionless) $\theta = -0.265$ and -0.765 , revealing the emergence of the SR phenomenon. At a threshold of 0.235, ρ decreases monotonically owing to the presence of a suprathreshold signal. The analytical solution qualitatively reproduces the experimental results. However, the experimental correlation coefficients are larger than the analytical ones over the whole range of σ_ξ . This seems to be due to the poor high-frequency characteristics of the fabricated OFET and thus a leakage of high-frequency components from the input signal [8].

Next, a robustness against external noise is evaluated using the derivative of the correlation coefficient [Eq. (3)] with respect to the external noise intensity, which is given by

$$\left| \frac{d\rho}{d\sigma_\xi} \right|^2 = \frac{D^2(1-D)^2}{\sigma_\xi^2} \times \left\{ \frac{2A\sigma_\xi^2 \left[\text{erf}\left(\frac{1}{\sqrt{2\sigma_{\theta+}^2}}\right) - \text{erf}\left(\frac{1}{\sqrt{2\sigma_{\theta-}^2}}\right) \right]}{(\text{var}[x] \text{var}[y])^{1/2}} + \left[5 - D \text{erf}\left(\frac{1}{\sqrt{2\sigma_{\theta+}^2}}\right) - (1-D) \text{erf}\left(\frac{1}{\sqrt{2\sigma_{\theta-}^2}}\right) \right] \times \left(\frac{4A^2\sigma_\xi^4 [E_+D + E_-(1-D)] \text{cov}[x, y]}{(\text{var}[x] \text{var}[y])^{3/2}} \right)^2 \right\}, \quad (5)$$

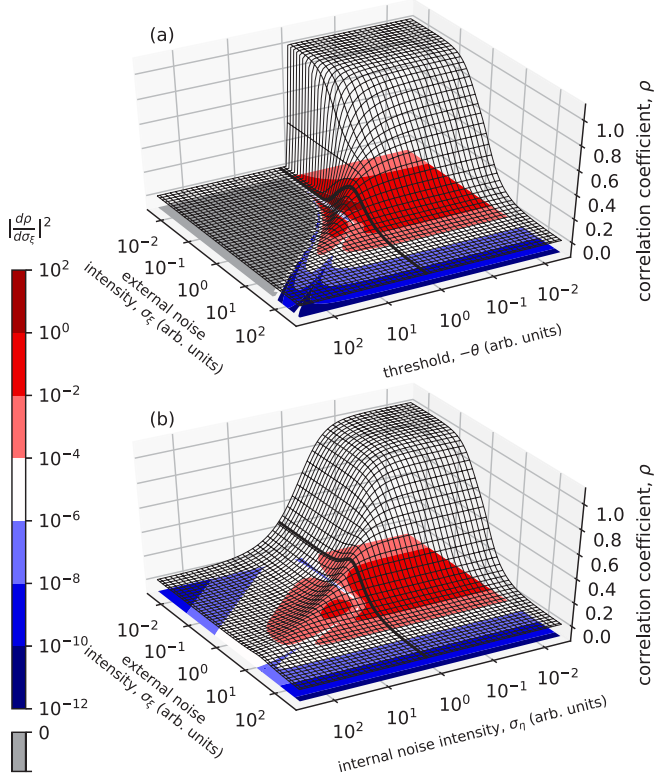


FIG. 2. Correlation coefficient between input and output signals (three-dimensional surface) and the square of its first derivative with respect to external noise intensity (contour map) as functions of external noise intensity and threshold at $\sigma_\eta = 0$ (a) and of external noise intensity and internal noise intensity at $\theta = 0$ (b) for the OFET model. Here, the duty ratio of the input signal $D = 80\%$ and the fitting parameter $A = 1$.

which becomes smaller as the signal transmission performance of the system is affected less by external noise.

III. RESULTS AND DISCUSSION

Figure 2(a) shows the variations of the correlation coefficient and the square of its derivative as functions of the external noise intensity and threshold, which are calculated using Eqs. (3) and (5). Bell-shaped curves of the correlation coefficient as a function of the external noise intensity [for example, a bold solid line in Fig. 2(a)] can be found only in the subthreshold region ($\theta < -1$), which is a fingerprint of the SR effect. In contrast, ρ decreases monotonically with external noise, and no SR can be seen in the suprathreshold region ($\theta > -1$). At small external noise intensity (e.g., $\sigma_\xi \leq 10^{-1}$), the high system performance ($\rho \approx 1$) at $\theta > -1$ drops abruptly to zero below the threshold of $\theta = -1$. A similar plot but with the threshold replaced by the internal noise intensity [Fig. 2(b)] shows similar qualitative behavior. When the internal noise intensity is large (e.g., $\sigma_\eta \geq 10$), the correlation coefficient shows a bell-shaped dependence on the external noise intensity [Fig. 2(b)] as well as a threshold dependence [Fig. 2(a)]. Furthermore, the large value of ρ (e.g., at $\sigma_\xi \leq 10^{-1}$ and $\sigma_\eta \leq 10^{-1}$) gradually falls to zero with increasing internal noise intensity. Thus, the internal noise intensity σ_η has a

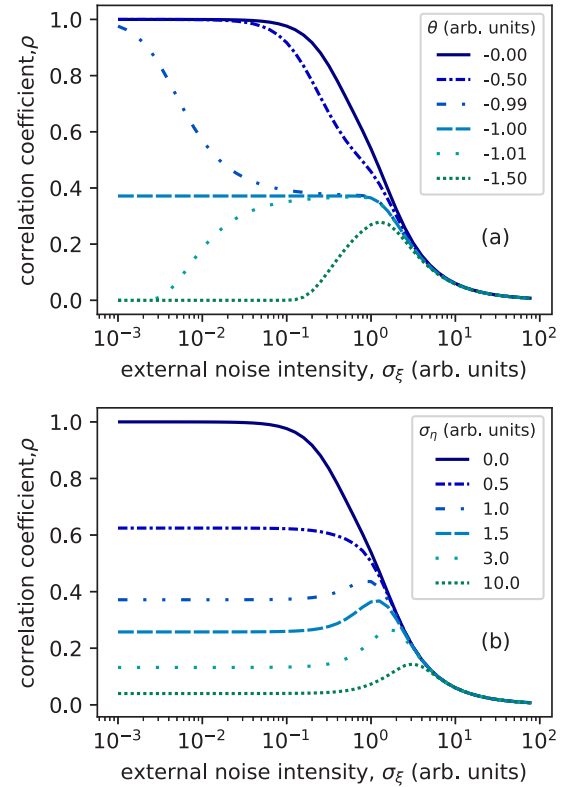


FIG. 3. Variation of the correlation coefficient between input and output signals as a function of external noise intensity for various values of threshold at internal noise intensity $\sigma_\eta = 0$ (a), and for various amplitudes of internal noise at threshold $\theta = 0$ (b). Here, duty ratio of input signal $D = 80\%$ and fitting parameter $A = 1$.

similar effect to that of the threshold θ for a nonlinear system. However, there is a remarkable difference in the behavior of the correlation coefficient with respect to variations in the value of the threshold near $\theta = -1$ [Fig. 3(a)]. On the other hand, the correlation coefficient remains unaffected by changes in the intensity of the external noise when the latter is less than about 0.1, regardless of the internal noise intensity [Fig. 3(b)]. Thus, the effect of external noise is influenced far more strongly by fluctuations in the threshold than by fluctuations in the intensity of internal noise. The formation of the plateau and the peak shift by internal noise, of the system performance with respect to external noise intensity, is shown in Fig. 3(b). This is similar to that by multiplicative noise in a bistable system (multiplicative SR) [24]. These are due to characteristics of noise that change a threshold (a barrier height of a potential), though internal noise in this paper makes a threshold higher whereas multiplicative noise in [24] moves the threshold in the opposite direction. As far as the derivative of ρ with respect to σ_ξ is concerned, a strong dependence on external noise (e.g., $|\frac{d\rho}{d\sigma_\xi}|^2 > 1$) can be found only in Fig. 2(a) (color bar). Furthermore, the region with $|\frac{d\rho}{d\sigma_\xi}|^2 = 0$ vanishes in Fig. 2(b) (color bar) owing to the presence of a broad peak in ρ resulting from its bell-shaped dependence on external noise. These results mean that internal noise plays a thresholdlike role for a nonlinear system with a weaker dependence on external noise than the conventional threshold.

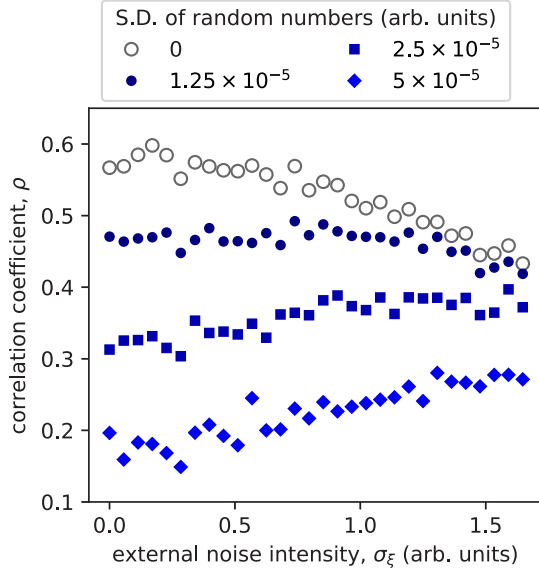


FIG. 4. Variation of the correlation coefficient between input and output signals as a function of external noise intensity when random numbers with a Gaussian distribution were added to the output signal. Symbols represent the averaged value of the correlation coefficient calculated from experimental data from four trials under identical conditions using the fabricated OFET (open circles) and with random numbers with different standard deviations added to the output signal (filled circles, squares, and diamonds). The normalized dimensionless parameters of the input signal intensity are threshold $\theta = 0.235$, internal noise intensity $\sigma_\eta = 1.25 \times 10^{-5}$, and fitting parameter $A = 1.2 \times 10^{-5}$.

According to the above results, SR should be observed on the addition of noise (as internal noise) subsequent to the output of signals from an OFET under a suprathreshold condition, where no SR can be observed in the absence of such noise. The noise added to the output signal has an equivalent role to that of internal noise because internal additive noise is independent of the input signal. In an OFET at a threshold $\theta = 0.235$, no gain in correlation coefficient was seen experimentally, as shown in Fig. 1. We evaluated the sum of the output signal from the OFET experiment and noise represented by random numbers with a Gaussian distribution and then calculated the correlation coefficient between the input and the summed signal (Fig. 4). With increasing standard deviation of the random numbers, the slope of the correlation coefficient changes from negative to positive as σ_ξ increases. In other words, adding noise to the output signal of the system leads to emergence of the SR phenomenon. This is because the addition of random numbers as internal noise transforms a suprathreshold input signal into a subthreshold one. From this, it follows that it should be possible to realize SR using the internal noise of an OFET and/or noise present between the OFET and a measuring instrument, even if the OFET is in a normally ON state (ON state at zero gate voltage) or threshold free. This can be implemented without dc bias tuning. Generally, OFETs are susceptible to shifts of threshold to the positive (for p -type FETs) caused by ambient air and increases in the OFF current [25–27]. Such threshold-free systems or nonlinear systems with suprathreshold signals can exhibit SR generated

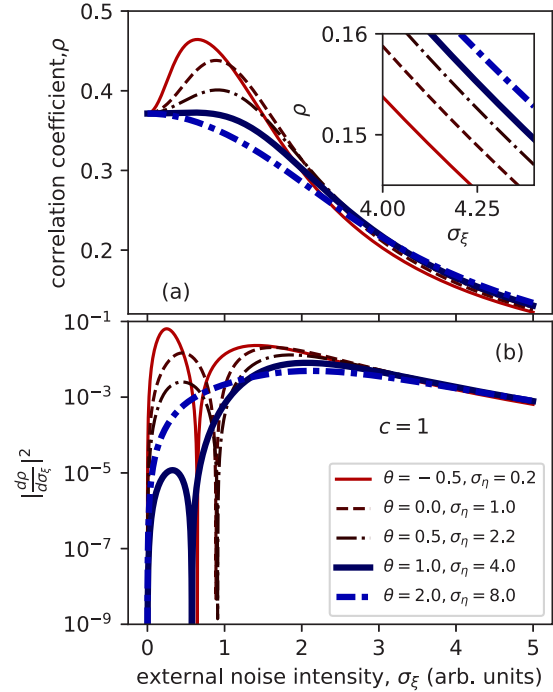


FIG. 5. Variation of the correlation coefficient between input and output signals (a) and the magnitude of its derivative with respect to external noise intensity (b) as functions of external noise intensity under the condition that the system shows identical signal transmission performance at $\sigma_\xi = 0$. Here, the duty ratio of input signal $D = 80\%$, the fitting parameter $A = 1$, and the constant $c = 1$ in Eq. (6).

by additional internal noise, consistent with the results of previous work [18]. Since we are dealing here with noise added to the output of a nonlinear response system as internal noise, it might be possible to control this internal noise after measuring the output signal. However, in other nonlinear systems, such as globally or locally coupled arrays [28,29], where internal noise is processed as input, it will be uncontrollable after measurement and will play a different role.

To evaluate the difference between threshold and internal noise, we determine appropriate conditions under which threshold and internal noise systems show identical signal transmission performance without the application of external noise.

We assume that ρ_0 (the correlation coefficient at $\sigma_\xi = 0$) is constant, and, from Eq. (4), obtain the condition

$$c = \text{const} = \begin{cases} \frac{4\theta^2}{\sigma_\eta^2} & (\theta \geq 1), \\ \frac{(-1-\theta)^4}{\sigma_\eta^2} & (-1 < \theta < 1), \end{cases} \quad (6)$$

where $c = \rho_0/[A\sqrt{D(1-D)(1-\rho_0^2)}]$. Figure 5 shows the correlation coefficient and $|d\rho/d\sigma_\xi|^2$ as functions of the external noise intensity using Eqs. (3)–(6). Furthermore, as the threshold and internal noise intensity increase, the peak in the correlation coefficient becomes smaller and broader, reducing the values of $|d\rho/d\sigma_\xi|^2$ except around the sharp dip. As the internal noise intensity σ_η increases or as the value of the threshold θ becomes more negative, the input signal wave becomes more deeply submerged below the subthreshold

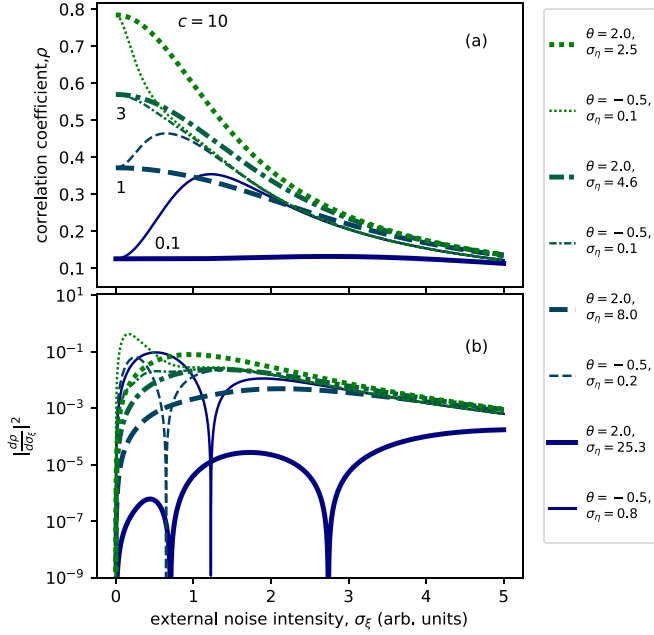


FIG. 6. Variation of the correlation coefficient between input and output signals (a) and a magnitude of its derivative of external noise intensity (b) as a function of external noise intensity for various constant values c in Eq. (6). Here, duty ratio of input signal $D = 80\%$ and fitting parameter $A = 1$.

region. Hence, in a nonlinear response system with large *positive* values of both θ and σ_η , the signal is affected predominantly by the internal noise rather than by the threshold. In brief, the use of internal noise instead of a threshold should allow suppression of fluctuations in system performance due to changes in external noise intensity (Fig. 5). This means that, through the internal noise effect, a system can acquire robust performance with respect to external fluctuations, in exchange for disappearance of the peak in ρ , namely, SR. Even if c (i.e., the correlation coefficient at $\sigma_\xi = 0$) is changed, variations in ρ are suppressed by the use of internal noise instead of a threshold, as shown in Fig. 6.

It is noteworthy that when the external noise intensity is large (e.g., $\sigma_\xi \geq 3$), there is a slight increase in the correlation coefficient when internal noise is used instead of a threshold [Fig. 5 (inset)]. This can be attributed to nonlocalized output of the system. In a system with lower internal noise, positive values of the output tend toward zero on the application of external noise as a result of frequent crossings of the threshold for input [Figs. 7(d) and 7(e)]. The convergence to zero of the output, which is otherwise positive, leads to a reduction in the differences among the mean values of the output for different values of the input signal. In contrast, in a system with large internal noise instead of a threshold, the positive values of the output do not tend to zero and remain broadly distributed [Figs. 7(b) and 7(c)]. For this reason, a system involving internal noise relatively easily generates different outputs for high and low inputs, and gives slightly better system performance than a threshold system with negligible internal noise when the distribution of external noise is large. This internal noise effect is observed in the system regardless of the value of c . For high c (e.g., $c = 10$), the performance of a

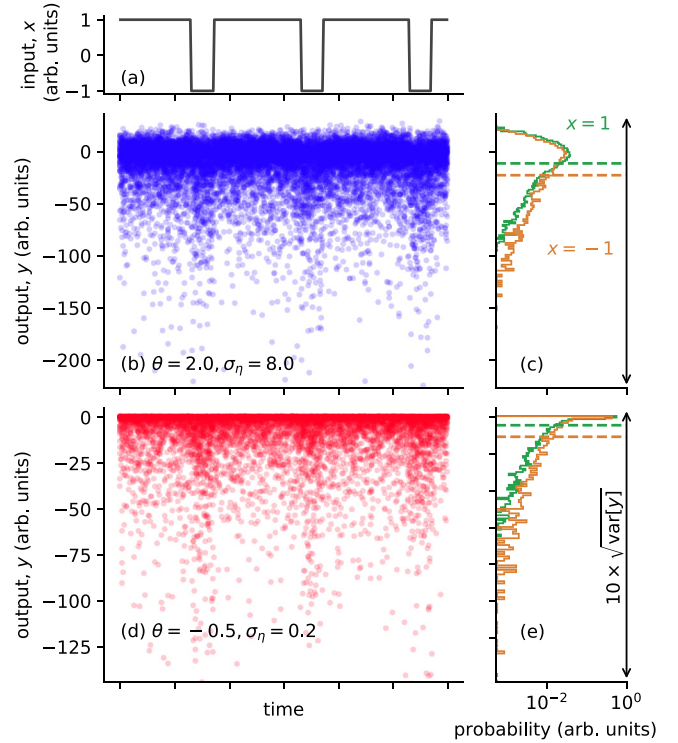


FIG. 7. Time courses of output value (b), (d) to input signal (a) calculated using Eq. (1) and output distribution (c), (e). A total of 5000 dots (100 dots \times 50 trials) are plotted per a period of input as output of OFET (b), (d). Output distribution is normalized and horizontal lines indicate the average value of output to each input signal value (c), (e). Here, external noise intensity $\sigma_\xi = 4$, duty ratio of input signal $D = 80\%$, and fitting parameter $A = 1$.

system utilizing internal noise instead of a threshold is better than that of a system with low internal noise for a wide range of external noise intensity (Fig. 6).

Here and in the previous study [8], we have assumed a white spectrum of the internal noise since the thermal noise derived from the capacitance of the OFET insulator is large in the system under study, namely, a common-drain circuit using the fabricated OFET and a load resistor. This thermal noise seems to predominate over noise derived from the semiconductor due to the small load resistance of the OFET circuit, which converts the source-drain current into an output voltage. Because semiconductor devices have $f^{-\gamma}$ ($\gamma \approx 1$) noise in most cases [22,23,30–32], the effect of such a noise spectrum on SR needs to be examined to allow proper utilization of the material characteristics of OFETs.

IV. CONCLUSION

In conclusion, we have addressed the use of an internal noise effect as a threshold for SR using an OFET model. Subthreshold conditions for the input signal, where SR is frequently observed, can be achieved by additive internal noise without changing the threshold or input dc bias. In accordance with this, additive noise allows generation of an SR effect on the experimentally measured output signal under suprathreshold conditions. This result shows that a condition

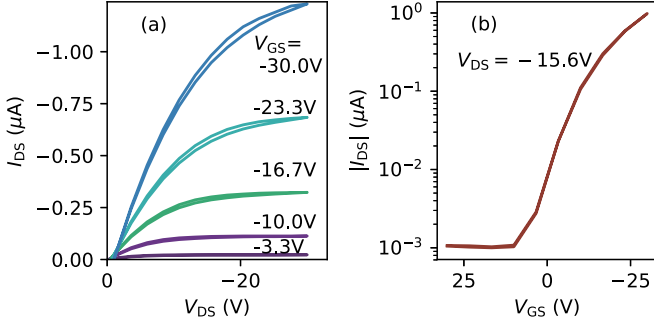


FIG. 8. Drain current vs drain voltage (a) and vs gate voltage (b) of the fabricated OFET.

equivalent to internal noise can be imposed from outside of the device. In a comparison between an internal noise system and a conventional threshold system with identical system performances in the absence of external noise, the former system is more robust against external noise and also has better signal transmission performance under conditions of large external noise.

APPENDIX A: FABRICATED OFET

A fabricated OFET is a top-gate bottom-contact structure using regioregular poly(3-hexylthiophene) and *a*-poly(methyl methacrylate) as a semiconductor and insulator, respectively. The fabricated OFET indicated typical transistor characteristics as shown in Fig. 8. The field-effect mobility and threshold of the OFET are $3 \times 10^{-3} \text{ cm}^2 \text{ V}^{-1} \text{ s}^{-1}$ (at $V_{DS} = -15.6 \text{ V}$) and -0.45 V , respectively. In Fig. 1, the experimental conditions with threshold values (signal-to-threshold distances) $\theta = 0.235$, -0.265 , and -0.765 were set up with input dc bias 0, -2.0 , and -4.0 V , respectively. For experimental details, see our previous study [8].

APPENDIX B: DERIVATION OF FORMULA

The correlation coefficient of input x and output signal y is expressed in the following:

$$\rho = \frac{\text{cov}[x, y]}{\sqrt{\text{var}[x]\text{var}[y]}} \quad (\text{B1})$$

$$= \frac{E[xy] - E[x]E[y]}{\sqrt{(E[x^2] - E[x]^2)(E[y^2] - E[y]^2)}}.$$

We have

$$E[x] = D - (1 - D) = -1 + 2D, \quad (\text{B2})$$

$$E[x^2] = D + (1 - D) = 1 \quad (\text{B3})$$

since $x = 1$ and -1 with the probability of D and $1 - D$, respectively.

1. Correlation coefficient for external noise existing

When external noise exists, the output of the OFET system is given by

$$y = \begin{cases} y_{\text{on}} = -A(x + \xi - \theta)^2 + \eta & (x + \xi < \theta) \\ y_{\text{off}} = \eta & (x + \xi \geq \theta), \end{cases} \quad (\text{B4})$$

where y_{on} and y_{off} are output signals at ON and OFF states, respectively. We assumed that external noise and internal noise have independent Gaussian distribution with zero mean and variance σ_ξ^2 and σ_η^2 , respectively. From (B4), the expected value of y given x is

$$\begin{aligned} E[y|x] &= E[y_{\text{on}}|x] \text{Prob}(x + \xi < \theta|x) \\ &\quad + E[y_{\text{off}}|x] \text{Prob}(x + \xi \geq \theta|x) \\ &= E[-A(x + \xi - \theta)^2|x] \text{Prob}(x + \xi < \theta|x) + E[\eta] \\ &= -A \int_{-\infty}^{-x+\theta} (x + \xi - \theta)^2 P(\xi) d\xi + E[\eta] \\ &= -A \sigma_\xi \frac{-x + \theta}{\sqrt{2\pi}} \exp\left(-\frac{(-x + \theta)^2}{2\sigma_\xi^2}\right) \\ &\quad + \frac{A}{2} [\sigma_\xi^2 + (-x + \theta)^2] \left[1 + \text{erf}\left(\frac{-x + \theta}{\sqrt{2}\sigma_\xi}\right)\right], \end{aligned} \quad (\text{B5})$$

where probability density function of external noise $P(\xi) = \exp[-\xi^2/(2\sigma_\xi^2)]/\sqrt{2\pi\sigma_\xi^2}$. The expected value of y^2 given x is

$$\begin{aligned} E[y^2|x] &= E[y_{\text{on}}^2|x] \text{Prob}(x + \xi < \theta|x) \\ &\quad + E[y_{\text{off}}^2|x] \text{Prob}(x + \xi \geq \theta|x) \\ &= E[A^2(x + \xi - \theta)^4 \\ &\quad - A(x + \xi - \theta)^2 \eta|x] \text{Prob}(x + \xi < \theta|x) + E[\eta^2] \\ &= A^2 \int_{-\infty}^{-x+\theta} (x + \xi - \theta)^4 P(\xi) d\xi \\ &\quad - A \int_{-\infty}^{-x+\theta} (x + \xi - \theta)^2 P(\xi) d\xi E[\eta] + \sigma_\eta^2 \\ &= A^2 \int_{-\infty}^{-x+\theta} (x + \xi - \theta)^4 P(\xi) d\xi + \sigma_\eta^2 \\ &= A^2 \sigma_\xi [(-x + \theta)^2 + 5\sigma_\xi^2] \frac{-x + \theta}{\sqrt{2\pi}} \\ &\quad \times \exp\left(-\frac{(-x + \theta)^2}{2\sigma_\xi^2}\right) \\ &\quad + \frac{A^2}{2} [(-x + \theta)^4 + 6(-x + \theta)^2 \sigma_\xi^2 + 3\sigma_\xi^4] \\ &\quad \times \left[1 + \text{erf}\left(\frac{-x + \theta}{\sqrt{2}\sigma_\xi}\right)\right] + \sigma_\eta^2. \end{aligned} \quad (\text{B6})$$

The expected values of y , y^2 , and xy are

$$E[y] = E[E[y|x]] = E[y|1]D + E[y|-1](1 - D), \quad (\text{B7})$$

$$\begin{aligned} E[y^2] &= E[E[y^2|x]] \\ &= E[y^2|1]D + E[y^2|-1](1 - D), \end{aligned} \quad (\text{B8})$$

$$E[xy] = E[xE[y|x]] = E[y|1]D - E[y|-1](1-D), \quad (\text{B9})$$

respectively. From (B2), (B5), (B7), and (B9), the covariance between x and y is

$$\begin{aligned} \text{cov}[x, y] &= E[xy] - E[x]E[y] \\ &= -2A\sigma_\xi^2 D(1-D)(E_+ - E_-), \end{aligned} \quad (\text{B10})$$

where

$$\begin{aligned} E_\pm &= \frac{1}{\sqrt{2\pi\sigma_{\theta\pm}^2}} \exp\left(-\frac{1}{2\sigma_{\theta\pm}^2}\right) \\ &+ \frac{1 + \sigma_{\theta\pm}^2}{2\sigma_{\theta\pm}^2} \left[1 + \text{erf}\left(\frac{1}{\sqrt{2\sigma_{\theta\pm}^2}}\right) \right], \end{aligned} \quad (\text{B11})$$

and

$$\sigma_{\theta\pm}^2 = \left(\frac{\sigma_\xi}{\mp 1 + \theta} \right)^2. \quad (\text{B12})$$

From (B2) and (B3), the variance value of x is

$$\text{var}[x] = E[x^2] - E[x]^2 = 4D(1+D). \quad (\text{B13})$$

From (B5), (B6), (B7), and (B8), the variance of y is

$$\begin{aligned} \text{var}[y] &= E[y^2] - E[y]^2 \\ &= A^2\sigma_\xi^4 \left\{ E_{2+}D + E_{2-}(1-D) \right. \\ &\quad \left. + \frac{\sigma_\eta^2}{A^2\sigma_\xi^4} - [E_+D + E_-(1-D)]^2 \right\}, \end{aligned} \quad (\text{B14})$$

where

$$\begin{aligned} E_{2\pm} &= \frac{1 + 5\sigma_{\theta\pm}^2}{\sqrt{2\pi\sigma_{\theta\pm}^6}} \exp\left(-\frac{1}{2\sigma_{\theta\pm}^2}\right) \\ &+ \frac{1 + 6\sigma_{\theta\pm}^2 + 3\sigma_{\theta\pm}^4}{2\sigma_{\theta\pm}^4} \left[1 + \text{erf}\left(\frac{1}{\sqrt{2\sigma_{\theta\pm}^2}}\right) \right]. \end{aligned} \quad (\text{B15})$$

From (B1), (B10), (B13), and (B14), we obtain

$$\begin{aligned} \rho &= -D(1-D)(E_+ - E_-) \\ &\times \left\{ \left[D(1-D) \left(E_{2+}D + E_{2-}(1-D) + \frac{\sigma_\eta^2}{A^2\sigma_\xi^4} \right. \right. \right. \\ &\quad \left. \left. - [E_+D + E_-(1-D)]^2 \right) \right]^{-1/2} \right\}. \end{aligned} \quad (\text{B16})$$

2. Correlation coefficient for no external noise

When no external noise exists with input signal, the expected value of y given x is

$$E[y|x] = E[-A(x - \theta)^2|x] \text{Prob}(x < \theta|x). \quad (\text{B17})$$

Therefore from (B7) we obtain

$$E[y] = \begin{cases} 0 & (\theta \leq -1) \\ A(-1 - \theta)^2(1-D) & (-1 < \theta \leq 1) \\ A(-1 - \theta)^2(1-D) + A(1 - \theta)^2D & (1 < \theta). \end{cases} \quad (\text{B18})$$

The expected value of y^2 given x is

$$E[y^2|x] = E[A^2(x - \theta)^4|x] \text{Prob}(x < \theta|x) + \sigma_\eta^2, \quad (\text{B19})$$

and we obtain from (B8)

$$E[y^2] = \begin{cases} \sigma_\eta^2 & (\theta \leq -1) \\ A^2(-1 - \theta)^4(1-D) + \sigma_\eta^2 & (-1 < \theta \leq 1) \\ A^2(-1 - \theta)^4(1-D) \\ \quad + A^2(1 - \theta)^4D + \sigma_\eta^2 & (1 < \theta) \end{cases} \quad (\text{B20})$$

and from (B9)

$$E[xy] = \begin{cases} 0 & (\theta \leq -1) \\ -A(-1 - \theta)^2(1-D) & (-1 < \theta \leq 1) \\ -A(-1 - \theta)^2(1-D) \\ \quad + A(1 - \theta)^2D & (1 < \theta). \end{cases} \quad (\text{B21})$$

From (B1), (B2), (B3), (B18), (B20), and (B21), the correlation coefficient between x and y at $\sigma_\xi = 0$ is

$$\rho_0 = \begin{cases} 0 & (\theta \leq -1) \\ \frac{(-1-\theta)^2 D(1-D)}{\sqrt{D(1-D)((-1-\theta)^4(1-D)D + \frac{\sigma_\eta^2}{A^2})}} & (-1 < \theta \leq 1) \\ \frac{4\theta D(1-D)}{\sqrt{D(1-D)(16\theta^2(1-D)D + \frac{\sigma_\eta^2}{A^2})}} & (1 < \theta) \end{cases}. \quad (\text{B22})$$

3. Differential value of correlation coefficient to external noise intensity

We have

$$\frac{d\rho}{d\sigma_\xi} = \frac{\partial\rho}{\partial\sigma_{\theta+}} \frac{d\sigma_{\theta+}}{d\sigma_\xi} + \frac{\partial\rho}{\partial\sigma_{\theta-}} \frac{d\sigma_{\theta-}}{d\sigma_\xi} + \frac{\partial\rho}{\partial\sigma_\xi}. \quad (\text{B23})$$

From (B11) we obtain

$$\begin{aligned} \frac{dE_\pm}{d\sigma_{\theta\pm}} &= \frac{-2}{\sqrt{2\pi\sigma_{\theta\pm}^4}} \exp\left(-\frac{1}{2\sigma_{\theta\pm}^2}\right) \\ &- \frac{1}{\sigma_{\theta\pm}^3} \left[1 + \text{erf}\left(\frac{1}{\sqrt{2\sigma_{\theta\pm}^2}}\right) \right], \end{aligned} \quad (\text{B24})$$

and from (B15)

$$\begin{aligned} \frac{dE_{2\pm}}{d\sigma_{\theta\pm}} &= \frac{-4(1 + 2\sigma_{\theta\pm}^2)}{\sqrt{2\pi\sigma_{\theta\pm}^8}} \exp\left(-\frac{1}{2\sigma_{\theta\pm}^2}\right) \\ &- 2 \frac{(1 + 3\sigma_{\theta\pm}^2)}{\sigma_{\theta\pm}^5} \left[1 + \text{erf}\left(\frac{1}{\sqrt{2\sigma_{\theta\pm}^2}}\right) \right]. \end{aligned} \quad (\text{B25})$$

Therefore from (B12) and (B16) the differential value of ρ to σ_ξ is

$$\frac{d\rho}{d\sigma_\xi} = \frac{-D(1-D)}{\sigma_\xi} \left\{ \frac{2A\sigma_\xi^2 \left[\operatorname{erf}\left(\frac{1}{\sqrt{2\sigma_{\theta+}^2}}\right) - \operatorname{erf}\left(\frac{1}{\sqrt{2\sigma_{\theta-}^2}}\right) \right]}{(\operatorname{var}[x]\operatorname{var}[y])^{1/2}} + \left[5 - D \operatorname{erf}\left(\frac{1}{\sqrt{2\sigma_{\theta+}^2}}\right) - (1-D) \operatorname{erf}\left(\frac{1}{\sqrt{2\sigma_{\theta-}^2}}\right) \right] \right. \\ \left. \times \left(\frac{4A^2\sigma_\xi^4 D(1-D)[E_+D + E_-(1-D)]\operatorname{cov}[x,y]}{(\operatorname{var}[x]\operatorname{var}[y])^{3/2}} \right) \right\}. \quad (\text{B26})$$

-
- [1] L. Gammaitoni, P. Hänggi, P. Jung, and F. Marchesoni, *Rev. Mod. Phys.* **70**, 223 (1998).
- [2] J. J. Collins, C. C. Chow, and T. T. Imhoff, *Nature (London)* **376**, 236 (1995).
- [3] S. M. Bezrukov and I. Vodyanoy, *Nature (London)* **378**, 362 (1995).
- [4] J. Levin and J. Miller, *Nature (London)* **380**, 165 (1996).
- [5] J. K. Douglass, L. Wilkens, E. Pantazelou, and F. Moss, *Nature (London)* **365**, 337 (1993).
- [6] D. F. Russell, L. A. Wilkens, and F. Moss, *Nature (London)* **402**, 291 (1999).
- [7] B. J. Gluckman, T. I. Netoff, E. J. Neel, W. L. Ditto, M. L. Spano, and S. J. Schiff, *Phys. Rev. Lett.* **77**, 4098 (1996).
- [8] Y. Suzuki, K. Matsubara, and N. Asakawa, *Appl. Phys. Lett.* **109**, 093702 (2016).
- [9] S. Kasai and T. Asai, *Appl. Phys. Express* **1**, 083001 (2008).
- [10] S. Kasai, K. Miura, and Y. Shiratori, *Appl. Phys. Lett.* **96**, 194102 (2010).
- [11] K. Nishiguchi and A. Fujiwara, *Jpn. J. Appl. Phys., Part 1* **50**, 06GF04 (2011).
- [12] I. Y. Lee, X. Liu, B. Kosko, and C. Zhou, *Nano Lett.* **3**, 1683 (2003).
- [13] I. Lee, X. Liu, C. Zhou, and B. Kosko, *IEEE Trans. Nanotechnol.* **5**, 613 (2006).
- [14] Y. Hakamata, Y. Ohno, K. Maehashi, S. Kasai, K. Inoue, and K. Matsumoto, *J. Appl. Phys.* **108**, 104313 (2010).
- [15] Y. Hakamata, Y. Ohno, K. Maehashi, K. Inoue, and K. Matsumoto, *Appl. Phys. Express* **4**, 045102 (2011).
- [16] T. Kanki, Y. Hotta, N. Asakawa, T. Kawai, and H. Tanaka, *Appl. Phys. Lett.* **96**, 242108 (2010).
- [17] N. Asakawa, K. Umemura, S. Fujise, K. Yazawa, T. Shimizu, M. Tansho, T. Kanki, and H. Tanaka, *J. Nanophotonics* **8**, 083077 (2014).
- [18] P. C. Gailey, A. Neiman, J. J. Collins, and F. Moss, *Phys. Rev. Lett.* **79**, 4701 (1997).
- [19] S. M. Bezrukov and I. Vodyanoy, *Nature (London)* **385**, 319 (1997).
- [20] N. G. Stocks, *Phys. Rev. Lett.* **84**, 2310 (2000).
- [21] F. Apostolico, L. Gammaitoni, F. Marchesoni, and S. Santucci, *Phys. Rev. E* **55**, 36 (1997).
- [22] R. Harsh and K. S. Narayan, *J. Appl. Phys.* **118**, 205502 (2015).
- [23] J. Rhayem, M. Valenza, D. Rigaud, N. Szydlo, and H. Lebrun, *J. Appl. Phys.* **83**, 3660 (1998).
- [24] L. Gammaitoni, F. Marchesoni, E. Menichella-Saetta, and S. Santucci, *Phys. Rev. E* **49**, 4878 (1994).
- [25] M. S. A. Abdou, F. P. Orfino, Y. Son, and S. Holdcroft, *J. Am. Chem. Soc.* **119**, 4518 (1997).
- [26] Y. Qiu, Y. Hu, G. Dong, L. Wang, J. Xie, and Y. Ma, *Appl. Phys. Lett.* **83**, 1644 (2003).
- [27] S. Hoshino, M. Yoshida, S. Uemura, T. Kodzasa, N. Takada, T. Kamata, and K. Yase, *J. Appl. Phys.* **95**, 5088 (2004).
- [28] K. Wiesenfeld, *Phys. Rev. A* **44**, 3543 (1991).
- [29] J. F. Lindner, B. K. Meadows, W. L. Ditto, M. E. Inchiosa, and A. R. Bulsara, *Phys. Rev. Lett.* **75**, 3 (1995).
- [30] S. Martin, A. Dodabalapur, Z. Bao, B. Crone, H. E. Katz, W. Li, A. Passner, and J. A. Rogers, *J. Appl. Phys.* **87**, 3381 (2000).
- [31] A. Carbone, B. K. Kotowska, and D. Kotowski, *Phys. Rev. Lett.* **95**, 236601 (2005).
- [32] Y. Song and T. Lee, *J. Mater. Chem. C* **5**, 7123 (2017).